

An Improved Torque Feed-forward Control with Observer-based Inertia Identification in PMSM Drives

Shouhua Zhao *, Yangcheng Chen * and Lin Cui *

Abstract - This paper is concerned with speed tracking control problem for permanent-magnet synchronous drives (PMSM) in the presence of an variable load torque and unknown model parameters. The disturbance of speed control caused by inaccuracy of model parameters has been investigated. A load torque observer has been proposed to observe the load torque and estimate the disturbance caused by inaccuracy of model parameters. Both inertia and friction coefficient are identified in gradient descent approach. The stability condition of the observer has also been studied. Furthermore an improved feed-forward control has been introduced to reduce the speed track error. The proposed control strategy has been verified by both simulation and experimental results

Keywords: Observer, Identification, Feed-forward, PMSM

1. Introduction

Servo control systems have been widely used in modern technology-intensive industrial control for advanced control performances. PMSM control systems have been attracting much attention for easier control realization and higher control precision than other servo system. It has become a hot topic to improve performance of PMSM control system under variable load and unknown system parameters. Recent years a large contribution has been made to improve transient and steady performances of PMSM control system. Ichiro Awaya has proposed a method of disturbance observing and identification of parameters in [1]. However the method has been limited to theory for its requirement of extra information, such as the period of reference speed as described in [2]. Kyo-Beum Lee has designed two separate observers to observe disturbance and inertia in [3]. Also in [4], relative higher control cost has been paid for realizing of neural network. Sheng-Ming Yang adopts algebraic method to get disturbance in identification of parameters in [5]. All these methods for observation and identification are limited to theory for the reasons—the period of reference speed must be a known quantity or control strategy is too complicated. How to release the

dependence on these extra conditions with satisfied performance is the main concern of this paper.

In this paper, the disturbance caused by inaccuracy of model parameters is analyzed in detail on the basis of plant model. It is estimated on the basis of the observer of load torque. The identification of inertia and friction coefficient in gradient descent approach has been realized. The stability of observer is analyzed and a condition to achieve the stability is provided. The torque feed-forward control strategy with correction of derivative of speed error is used to reduce the speed track error and improve the system dynamic performance. In the end, both simulation and experimental results are presented to verify the proposed control strategy.

2. Model Disturbance Analysis

To simplify the analysis, Fig.1 shows dynamic model of a mechanical system,

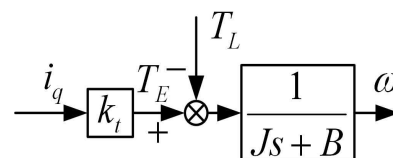


Fig. 1. Dynamic model of a mechanical system

* College of Electrical Engineering, Zhejiang University
(zxz_9999@163.com,yschen@zju.edu.cn, cl.ruohai@163.com)
Received 21 December 2012; Accepted 28 January 2013

where ω is mechanical angular speed of rotor, T_E is the electromagnetic torque, T_L is the load torque, J is the inertia of system, B is the friction coefficient, i_q is the q-axis current, k_t is the torque constant coefficient.

It is assumed that the motor is connected with external mechanical device with a rigid couple-link. Since the sample frequency of the control system is very high, the load torque T_L can be treated as constant in a short interval. Based on the above assumptions, the state equations of system model can be formulated in (1) and (2).

$$\frac{d\omega}{dt} = \frac{1}{J} T_E - \frac{B}{J} \omega - \frac{1}{J} T_L \quad (1)$$

$$\frac{dT_L}{dt} = 0 \quad (2)$$

The total disturbance of torque T_{dis} consists of the load torque T_L and the model disturbance T_{mdis} caused by inaccuracy of model parameters. So if T_{mdis} can be separated from the total disturbance T_{dis} , the system parameters that cause T_{mdis} may be identified. The relation between T_{mdis} and T_L can be written as

$$T_{dis} = T_{mdis} + T_L \quad (3)$$

$$\begin{aligned} T_E &= J \frac{d\omega}{dt} + B\omega + T_L \\ &= \hat{J} \frac{d\omega}{dt} + \hat{B}\omega + \Delta J \frac{d\omega}{dt} + \Delta B\omega + T_L \end{aligned} \quad (4)$$

$$T_{mdis} = \Delta J \frac{d\omega}{dt} + \Delta B\omega = T_E - \hat{J} \frac{d\omega}{dt} - \hat{B}\omega - T_L \quad (5)$$

$$J = \hat{J} + \Delta J, \quad B = \hat{B} + \Delta B \quad (6)$$

where, J and B denote the nominal value of inertia and friction coefficient respectively, \hat{J} and \hat{B} used in equation are identified values of J and B respectively, which means that T_{mdis} is caused by error ΔJ and ΔB . The discrete form of (5) is formulated in (7).

$$\left[\frac{J}{T_s} - \left(\frac{J}{T_s} - B \right) z^{-1} \right] \omega(k) = T_E(k-1) - T_L(k-1) - T_{mdis}(k-1) \quad (7)$$

3. Estimation of Model Disturbance Based on Load Torque Observer

Base on (1) and (2), the observer of T_L can be established in (8) [5, 6, 7].

$$\bar{\hat{x}}(k+1) = A\bar{\hat{x}}(k) + bu(k) + K(y(k) - \hat{y}(k)) \quad (8)$$

$$\bar{\hat{x}}(k) = \begin{bmatrix} \hat{\omega}(k) & \hat{T}_L(k) \end{bmatrix}^T$$

$$u(k) = T_E(k), \quad y(k) = \omega(k)$$

$$A = \begin{bmatrix} 1 - \frac{T_s \hat{B}}{J} & -\frac{T_s}{J} \\ 0 & 1 \end{bmatrix}, \quad b = \begin{bmatrix} \frac{T_s}{J} \\ 0 \end{bmatrix}, \quad C = \begin{bmatrix} 1 \\ 0 \end{bmatrix}^T, \quad K = \begin{bmatrix} k_1 T_s \\ k_2 T_s \end{bmatrix}$$

where, K is the gain matrix of observer, T_s is the sample period.

The observability of system in (1) and (2) can be judged by the criterion as in (9).

$$\text{rank}(M) = \text{rank} \begin{bmatrix} C \\ CA \end{bmatrix} = \text{rank} \begin{bmatrix} 1 & 0 \\ 1 - \frac{T_s \hat{B}}{J} & -\frac{T_s}{J} \end{bmatrix} = n = 2 \quad (9)$$

Obviously, the observer in (8) meets the criterion in (9). The observer equation of angular speed is rearranged as

$$\begin{aligned} \left[\frac{\hat{J}}{T_s} - \left(\frac{\hat{J}}{T_s} - \hat{B} \right) z^{-1} \right] \hat{\omega}(k) &= T_E(k-1) - \hat{T}_L(k-1) \\ &+ k_1 \hat{J} (\omega(k-1) - \hat{\omega}(k-1)) \end{aligned} \quad (10)$$

The block diagram of proposed observer is shown in Fig. 2.

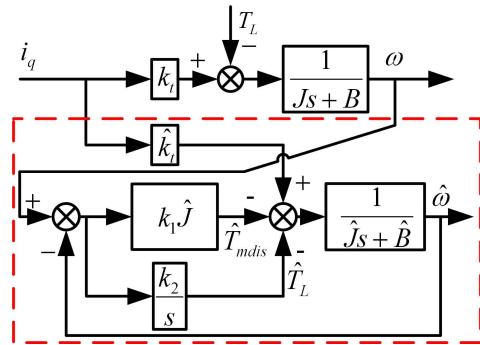


Fig. 2. The block diagram of observer

Comparing (10) with (7), the estimation of the model disturbance \hat{T}_{mdis} can be given in (11).

$$\hat{T}_{mdis}(k-1) = -k_1 \hat{J} (\omega(k-1) - \hat{\omega}(k-1)) \quad (11)$$

From the above analysis, disturbance caused by parameter errors can be estimated by load torque observer, which makes identification of inertia and friction coefficient possible.

4. Identification of Inertia and Friction Coefficient

In Part III, the estimation of model disturbance T_{mdis} has been derived from the observer of load torque.

It can be seen in (5) that the model disturbance T_{mdis} is caused by the inaccuracy of inertia and friction coefficient. So the next step is to find an adjustment rule as a function of \hat{J} and \hat{B} . The rule should make the objective function in (12) minimized.

$$j = \frac{1}{2} \int_0^t \hat{T}_{dms}^2 d\tau \quad (12)$$

In this paper, the gradient descent approach is applied to achieve the target. The parameters should be adjusted in the direction of minus gradient. The correction of variables can be formulated in (13) and (14).

$$\Delta J = -\lambda_J \int_0^t \hat{T}_{mdis} \frac{\partial \hat{T}_{mdis}}{\partial \hat{J}} d\tau \quad (13)$$

$$\Delta B = -\lambda_B \int_0^t \hat{T}_{mdis} \frac{\partial \hat{T}_{mdis}}{\partial \hat{B}} d\tau \quad (14)$$

Where, λ_J and λ_B are the gains of adjustment. ∂ denotes partial differential. The partial differential can be taken from (5).

Taking $\partial T_{mdis} / \partial \hat{J} = d\omega / dt = a$, $\partial T_{mdis} / \partial \hat{B} = \omega$ into (13) and (14), rearrangement of (13) and (14) can be formulated in (15) and (16).

$$\hat{J} = \frac{\lambda_J}{s} \hat{T}_{mdis} a + \hat{J}_0 \quad (15)$$

$$\hat{B} = \frac{\lambda_B}{s} \hat{T}_{mdis} \omega + \hat{B}_0 \quad (16)$$

The discrete form of (15) and (16) are formulated in (17) and (18).

$$\begin{aligned} \Delta J(k) &= \Delta J(k-1) + \lambda_J T_s \hat{T}_{mdis}(k-1) a(k-1) \\ \hat{J}(k) &= \hat{J}_0 + \Delta J(k) \end{aligned} \quad (17)$$

$$\begin{aligned} \Delta B(k) &= \Delta B(k-1) + \lambda_B T_s \hat{T}_{mdis}(k-1) \omega(k-1) \\ \hat{B}(k) &= \hat{B}_0 + \Delta B(k) \end{aligned} \quad (18)$$

The diagram block of identification is shown in Fig.3. It can be seen in Fig. 3 that both the inertial and friction coefficient identifications have a similar structure, except the input variables are different and the gains of adjustment may be different too.

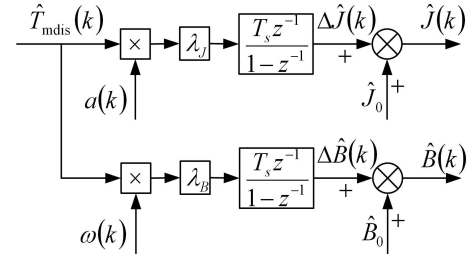


Fig. 3. The block diagram of parameters identification

According to the above analysis, the whole system can be expressed as,

$$\begin{aligned} \hat{\omega}(k) &= \left(1 - \frac{T_s \hat{B}}{\hat{J}}\right) \hat{\omega}(k-1) + \frac{T_s}{\hat{J}} T_E(k-1) \\ &\quad - \frac{T_s}{\hat{J}} \hat{T}_L(k-1) + k_1 T_s (\omega(k-1) - \hat{\omega}(k-1)) \end{aligned} \quad (19)$$

$$\hat{T}_L(k+1) = \hat{T}_L(k) + k_2 T_s (\omega(k) - \hat{\omega}(k)) \quad (20)$$

$$\hat{T}_{mdis}(k) = -k_1 \hat{J}(k-1) (\omega(k) - \hat{\omega}(k)) \quad (21)$$

$$\Delta J(k+1) = \Delta J(k) + \lambda_J T_s \hat{T}_{dms} a(k) \quad (22)$$

$$\Delta B(k+1) = \Delta B(k) + \lambda_B T_s \hat{T}_{dms}(k) \omega(k) \quad (23)$$

5. Condition of Stability of System

Containing uncertain load and unknown parameters, system is considered as a nonlinear system. Normally, the speed loop is slower than the current loop, and the parameter identification process is slower than the speed loop. So it is assumed that the identified parameters keep constant in a short interval. Then condition of stability can be analyzed as follows.

To be more generalized, Eq (1) is rewritten as

$$\dot{x} = bu + b_1 x + f(t) \quad (24)$$

In (24), x denotes ω . b denotes $1/J$. b_1 denotes $-B/J$. $f(t)$ means unknown load, and the derivative of $f(t)$ meets condition: $|\dot{f}(t)| \leq L \leq +\infty$ [8].

The observer in (8) can be rewritten as

$$\dot{\hat{x}} = bu + b_1\hat{x} + \hat{\sigma} + \frac{\alpha_1}{\varepsilon}(x - \hat{x}) \quad (25)$$

$$\dot{\hat{\sigma}} = \frac{\alpha_2}{\varepsilon^2}(x - \hat{x}) \quad (26)$$

where, $\hat{\sigma}$ is the observing variable of $f(t)$, and \hat{x} is the observing variable of ω , and $\varepsilon > 0$.

Then the state space equation of error system can be defined as follows:

$$\varepsilon \dot{\bar{\eta}} = \bar{A} \bar{\eta} + \bar{b} \dot{f} \quad (27)$$

where,

$$\eta_1 = \frac{x - \hat{x}}{\varepsilon}, \eta_2 = f(t) - \hat{\sigma}$$

$$\bar{A} = \begin{bmatrix} -\alpha_1 + b_1\varepsilon & 1 \\ -\alpha_2 & 0 \end{bmatrix}, \bar{b} = \begin{bmatrix} 0 \\ 1 \end{bmatrix}$$

The characteristic equation of (27) is expressed as

$$\lambda^2 + (\alpha_1 - b_1\varepsilon)\lambda + \alpha_2 = 0 \quad (28)$$

α_1 and α_2 should be selected to guarantee the matrix \bar{A} as Hurwitz. So if the matrix Q is positive definite, there is a matrix P satisfying the Lyapunov function in (29).

$$P\bar{A} + \bar{A}^T P = -Q \quad (29)$$

Defining Lyapunov function in (30),

$$V_0 = \varepsilon \bar{\eta}^T P \bar{\eta} \quad (30)$$

Then,

$$\begin{aligned} \dot{V}_0 &= \varepsilon \dot{\bar{\eta}}^T P \bar{\eta} + \varepsilon \bar{\eta}^T P \dot{\bar{\eta}} \\ &= (\bar{A} \bar{\eta} + \bar{b} \dot{f})^T P \bar{\eta} + \bar{\eta}^T P (\bar{A} \bar{\eta} + \bar{b} \dot{f}) \\ &= -\bar{\eta}^T Q \bar{\eta} + 2\bar{\eta}^T P \bar{b} \dot{f} \\ &\leq -\lambda_{\min}(Q) \|\bar{\eta}\|^2 + 2\varepsilon L \|P\bar{b}\| \|\bar{\eta}\| \end{aligned} \quad (31)$$

where, $\lambda_{\min}(Q)$ is the minimum eigenvalue of \bar{A} . The convergence condition of error system is determined by $\dot{V}_0 \leq 0$, which can be transformed into inequality in (32).

$$\|\bar{\eta}\| \leq \frac{2\varepsilon L \|P\bar{b}\|}{\lambda_{\min}(Q)} \quad (32)$$

If the initial states of observer are different from the initial states of plant, the observed variables will generate impulse phenomenon with small value of ε , which may degrade convergence of variables. So ε can be designed time-variant and continuous time piecewise function.

6. Feed-Forward Control Design

After the inertial and friction coefficient identified and load observed, a torque feed-forward control is used to improve the system dynamic performance and reduce the speed track error.

A simple way to implement the torque feed-forward control is to add a i_q reference component, which is calculated by the mechanical equation in (1) [9,10]. However there are some problems in practice, mainly due to speed ripple and feed-forward lag effect, since the phase of speed acceleration is lagged because of series of low-pass digital filters. The lag of acceleration is shown in Fig. 4.

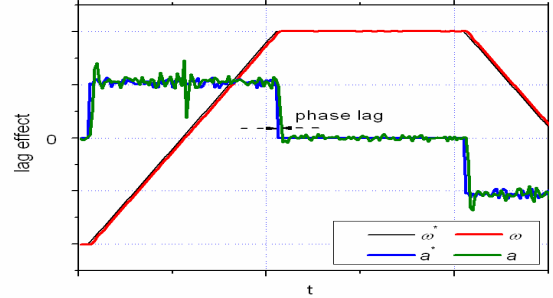


Fig. 4. Lag effect of acceleration

In Fig. 4, the speed calculated acceleration a lags behind reference speed acceleration a^* . And there is an large acceleration ripple due to the speed ripple and digital error. The direct use of acceleration may cause large ripple in i_q reference, which is unacceptable in a servo drive.

However, if the acceleration of reference speed is used to replace that of the calculated actual speed, the lag effect and the ripple due to speed acceleration can be eliminated. But if there is a speed overshoot, the acceleration of reference speed can not reflect the actual acceleration, which may deteriorate the problem. Fig. 5 shows the acceleration of reference speed a^* , derivative of speed error $d\omega_{error}$ and q-axial current i_q .

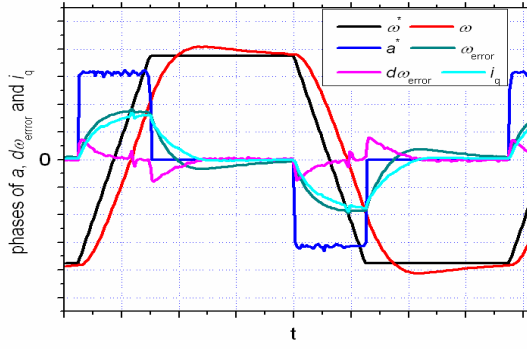


Fig. 5. Tracking control and tracking error

In Fig. 5, if the torque feed-forward control using the acceleration of reference speed is carried out, the speed error during acceleration and deceleration period will be decreased. But the large speed overshoot can't be overcome for the reason that there is a difference between the acceleration of actual speed and reference during overshoot, the acceleration of reference speed becomes zero. Then the term Ja^* makes no contribution.

To solve the problem, the derivative of error $d\omega_{error}$ can be introduced to correct the acceleration of reference speed. So the q-axis current termed by i_q^* is calculated as,

$$\begin{aligned} i_q^* &= i_{q_PI}^* + i_{feed_forward} \\ &= i_{q_PI}^* + \frac{k_f}{\hat{k}_t} \left(\hat{J} \left(\frac{d\omega_{ref}}{dt} + k_c \frac{d\omega_e}{dt} \right) + \hat{B}\omega + \hat{T}_L \right) \end{aligned} \quad (33)$$

where, $i_{q_PI}^*$ is generated by the speed PI controller, $i_{feed_forward}$ is the term of feed-forward current, k_c denotes the gain of compensation for acceleration, k_f is the gain of torque feed-forward current.

According to the simulation and experimental studies, the recommended value of k_f is 0.3~0.9, k_c is 0.1~0.3.

7. Simulation and Experiments

7.1. Simulation analysis

On the basis of above analysis, a simulation model has been created on the platform of Matlab\simulink. In the simulation, a trapezoidal waveform speed reference is used, with the acceleration of slope 1000rpm in 20ms. The specification of PMSM for simulation is shown in Table 1.

Table 1. Motor parameters for simulation

Parameter	Value
Nominal power (kW)	$P_n = 1$
Nominal speed(RPM)	$\omega_n = 2000$
Nominal torque (N·m)	$T_n = 4.7$
Number of pole pairs	$p = 4$
Inductance in d-axis (H)	$L_d = 5.51 \cdot 10^{-3}$
Inductance in q-axis (H)	$L_q = 10.77 \cdot 10^{-3}$
Armature winding resistance (Ω)	$R = 0.48$
Flux linkage of rotor permanent magnet(V/rad/s)	$\lambda_m = 0.4475$

Fig.6 shows the simulation results of parameters identification and load observation. In the beginning of simulation $t=0$, the observer is started, which will be stable in about 0.25s. At 0.65s, there is a load transient, and all parameters is changed, including J and B .

When the load step occurs, the observation of T_L and the identification of J responded rapidly. This is the worst case since all parameters are changed. The respond of identification of friction coefficient B delays for a while, which also happen at the start of the simulation. This phenomenon is caused by two factors that the initial acceleration is large and the term $J d\omega/dt$ is dominated. $B\omega$ will become effective when the speed is stable and acceleration is low. Then it will converge to a steady state, and close to its nominal value.

An overshoot of \hat{T}_L occurring at the load step is due to the fact that J and B all changed at same time, clearly which is the worst phenomenon. It also provides the evidence that the convergence of observing is quicker than that of parameters identification. To reduce the overshoot, a small value of the observer gain k_2 may be chosen.

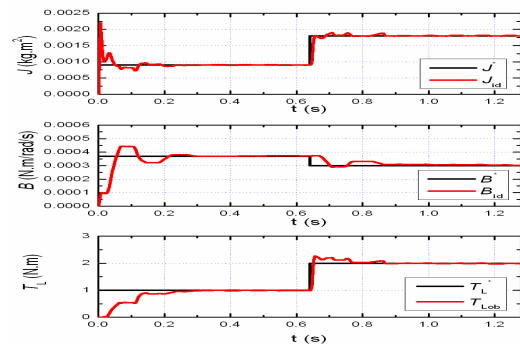


Fig. 6. Performance with inertia step and outside disturbance step

7.2. Experimental studies

The test platform consists of drive motor, load motor and an inertia disc. A rigid couple link is installed between drive motor and the load, which is shown in Fig. 7. The drive motor is a PM servo motor with the frame size 130mm and rated power of 1.0kW.

The drive used for test is based on a TMS320F2812 DSP with the rated power of 1.5kW.

In the test, the trapezoidal waveform reference speed is used, with the slope acceleration 3000rpm within 100ms. The gains of the observer and identification are chosen as follows: $k_1=20$, $k_2=-16$, $k_c=0.1$, $k_f=0.9$, $\lambda_j=0.45$, $\lambda_B=0.9$, $\varepsilon=1$.

The specifications of PMSM drive system are summarized in Table II along with their respective values.

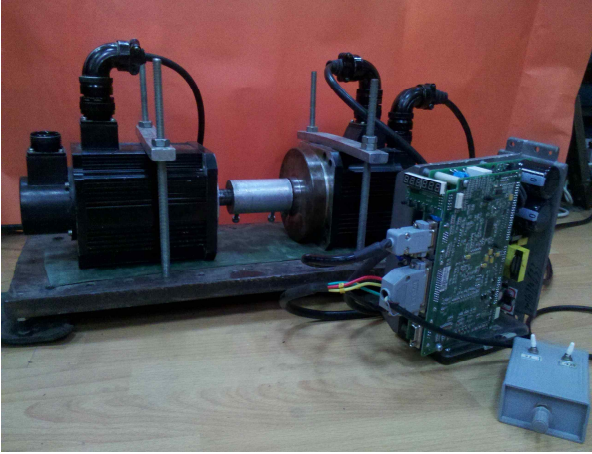


Fig. 7. The test platform

Table 2. Motor parameters for experiments

Parameter	Value
Nominal power (kW)	$P_n = 1$
Nominal speed(RPM)	$\omega_n = 2000$
Nominal torque (N·m)	$T_n = 4.7$
Number of pole pairs	$p = 4$
Inductance in d-axis (H)	$L_d = 13.2 \cdot 10^{-3}$
Inductance in q-axis (H)	$L_q = 17.3 \cdot 10^{-3}$
Armature winding resistance (Ω)	$R = 3.2$
Flux linkage of rotor permanent magnet(V/rad/s)	$\lambda_m = 0.9835$
Rotor and load inertia (kg.m ²)	$J = 8.5 \cdot 10^{-3}$
Friction coefficient (N·m/rad/s)	$B = 7.0 \cdot 10^{-3}$

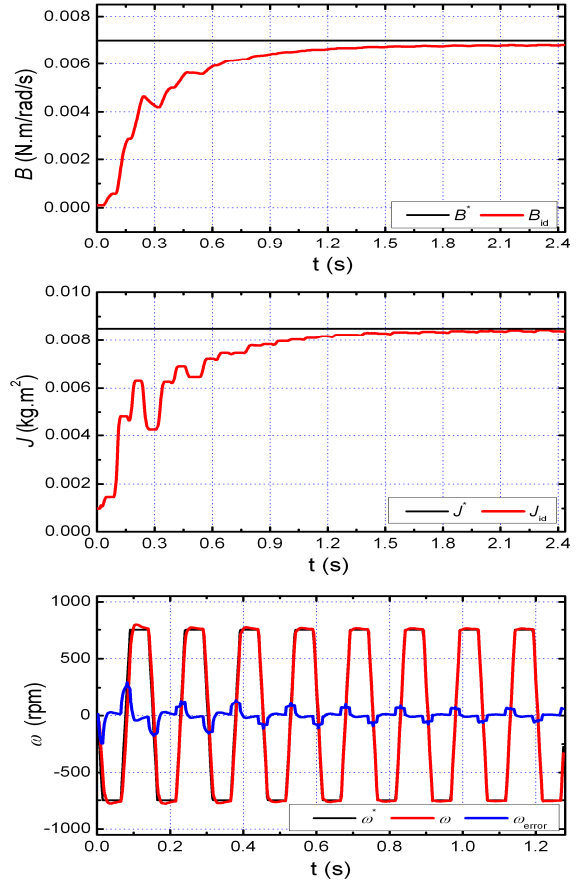


Fig. 8. Identification of parameters and speed tracking control with proposed feed-forward method

The identified system inertia J_{id} converges asymptotically to its nominal inertia J^* , the total inertia of system. In the identification of inertia, a vibration appears from 0.2s to 0.4s, which is caused by several factors, such as λJ , acceleration of speed and the tracking error etc. In the beginning of the test from $t=0$ to about $t=0.2s$, the identification of inertia and friction coefficient converged rapidly from 0 to their stable states. Then the convergence process slowed down. At about 1.8s, identification of parameters was stabled. It can be seen In Fig. 8, the speed tracking error ω_{error} is reduced in rapidly in the first two speed periods, in less than 0.2s, which can be explained by the relatively fast convergence of parameters identification. After the first two periods, the speed tracking error ω_{error} is reduced gradually along with the identification of inertia and friction coefficient. The performance of original speed PI controller will also affect the system performance even with torque feed-forward controller added. To demonstrate effectiveness of the proposed strategies, both terrible cases with poor PI control parameters are

considered- under damping with very large overshoot and over damping with very slow transient process. However, the system control performance can be improved significantly by the proposed torque feed-forward control. Figs. 9 and 10 show the speed tracking performance of the test system with and without the torque feed-forward control. In this test, the feed-forward gain k_f is set to 0.7, which means that 70 percentage of load torque is fed to system.

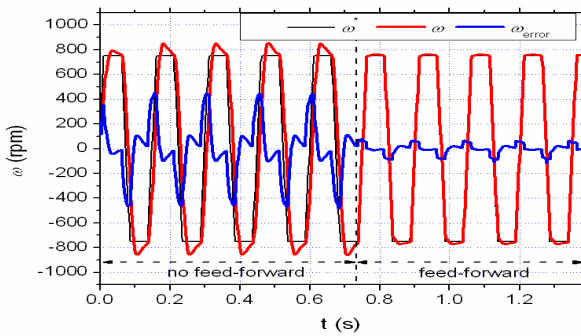


Fig. 9. The proposed feed-forward controls under speed overshoot condition

It can be seen in Fig. 9 that there is a large overshoot with original PI controller and the speed tracking error ω_{error} is large. However after the feed-forward control takes effective at about 0.7s, and the feed-forward current calculated by (33) is added to q-axis current reference, the speed overshoot is eliminated.

Fig. 10 shows a comparison between with and without feed-forward control, when there is an over damped respond in the speed with the original PI controller.

In Fig. 10, it can be seen that before feed-forward control, the speed tracking error ω_{error} is large too. However after feed-forward current is added at about 0.7s, the speed tracking error is reduced and the speed follows the speed reference perfectly.

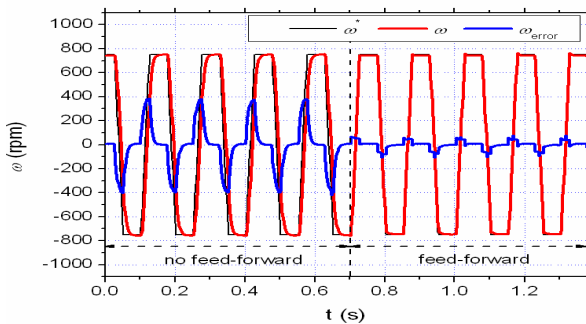


Fig. 10 Feed-forward under over damping condition

The results of simulation and experimental results have proven that the proposed observer-based identification and the improved feed-forward control can enhance system dynamic performance significantly, especially the transient performances including tracking error and setting time.

According to simulation and experiments above, the new control strategy is proved to be feasible for observing load and identifying of parameters. And the new proposed feed-forward control method is able to improve system dynamic performance.

8. Conclusion

This paper has illustrated an example of the application of observer in load torque observing and identification of mechanical parameters to motion control. The observer separates disturbance caused by inaccuracy of model parameters from the observed load torque. Both inertia and friction coefficient are identified in gradient descend approach. The proposed scheme does not need period of reference speed, or any time information of transient state and steady state of system. The required information about load torque and parameters is reconstructed by the observer of load torque. The stability condition of observer is given via Lyapunov stability theory. The proposed torque feed-forward control strategy with correction of derivative of speed error avoids the problem of phase lag and speed ripple effect.

The simulation and experimental results demonstrate that the novel control strategy has satisfied convergence property in identification of parameters and observation of load torque, which can also offer a reference in practice.

References

- [1] I. Awaya, Y. Kato, I. Miyake, and M. Ito, "New motion control with inertia identification function using disturbance observer," in *Proc. Power Electron. Motion Control Conf.*, 1992, pp. 77–81.
- [2] Shuai Du, Shouhua Zhao and Yangsheng Chen, "Inertia identification for speed control of PMSM servo motor", *ICEMS, 2011 International Conference*, July 2011. pp.1-6.
- [3] K.B. Lee, J.Y. Yoo, J.H. Song and I.Choy, "Improvement of low speed operation of electric machine with an inertia identification using RORLO," in *IEE Proc.-Electr. Power Appl.*, Vol. 151, no. 1, January 2004. pp. 116-120.
- [4] Kyo-Beum Lee and Frede Blaabjerg, "Robust and stable disturbance observer of servo system for low-speed operation," in *IEEE transactions on industry and applications*, Vol. 43, no. 3, May/June 2007. pp. 627-635.

- [5] S. M. Yang and Y. J. Deng, "Observer-based inertia identification for autotuning servo motor drives," in *Conf. Rec. 40th IEEE IAS Annu. Meeting*, 2005, pp. 968–972.
- [6] Shihua Li and Zhigang Liu, "Adaptive speed control for permanent-magnet synchronous motor system with variations of load inertia," in *IEEE transactions on industrial electronics*, vol. 56, no.8. August 2009, pp. 3050-3059.
- [7] Guchuan Zhu, Louis-A. Dessaint, Ouassima Akhrif and Azeddine Kaddouri, "Speed Tracking Control of a Permanent-Magnet Synchronous Motor with State and Load Torque Observer," in *IEEE transactions on industrial electronics*, vol. 47, no. 2, April 2000. Pp.346-355.
- [8] Xinhua Wang, Zengqiang Chen and Zhuzhi Yuan, "Output tracking based on extended observer for nonlinear uncertain systems," in *Control and Design*, vol. 19. no. 10, Oct 2004. pp. 1113-1116.
- [9] Kiyoshi Ohishi, Masato Nakao and Kouhei Ohnishi eatl, "Microprocessor- controlled dc motor for load-intensive position servo system," in *IEEE transactions on industrial electronics*, vol. IE-34, no. 1, February 1987. pp. 44-49.
- [10] Wei-sheng H, Chun-wei L and Pau-Lo H eatl, "Precision control and compensation of servomotors and machine tools via the disturbance observer," in *IEEE transactions on industrial electronics*, vol. 57, no. 1, January 2010. pp. 420-429.



Yangsheng Chen received the B.S. degree and M.S. degree in college of electrical engineering from Zhejiang University, Zhejiang, China, and Ph.D. degree in department of electric and electrical engineering from University of Sheffield, UK, in 1991, 1994 and 1999,

respectively.

He was a principal engineer in CT and TRW, where he led many significant projects, including high power density motor for industrial robots, aero electrical drive system for flight control, development of servo motor for ABS/EPS/ABC system in automobile, research of ECU and sensors. He is currently a professor in college of electrical engineering, Zhejiang University. His research interests include permanent magnet synchronous control, application of power electronics, motor design for automobile and related control system, motor electromagnetism theory, research of motor vibration and noise.



Shouhua Zhao received the B.S. degree and the M.S. degree in control science and engineering school from University of Jinan, Shandong, China, in 2007 and 2010, respectively. He is currently working toward the Ph.D. degree in College of Electrical Engineering, Zhejiang University, Zhejiang, China.

His research interest includes motion control, system identification and adaptive control in PMSM drives.



Lin Cui received the B.S. degree in electrical engineering from Xi'an Jiaotong University, Xi'an, China, in 2009, and is working toward the M.S. degree in College of Electrical Engineering, Zhejiang University, Zhejiang, China.

Her research interests include servo motion control, Fuzzy PID control and performance optimization of Servo system.